AAS 13-414

TRAJECTORY EXPLORATION WITHIN BINARY SYSTEMS COMPRISED OF SMALL IRREGULAR BODIES

Loic Chappaz* **and Kathleen Howell†**

In an initial investigation into the behavior of a spacecraft near a pair of irregular bodies, consider three bodies (one massless). Two massive bodies form the primary system that is comprised of an ellipsoidal primary (P_1) and a second spherical primary (P_2). Two primary configurations are addressed: 'synchronous' and 'non-synchronous'. Concepts and tools similar to those applied in the Circular Restricted Three-Body Problem (CR3BP) are exploited to construct periodic trajectories for a third body in synchronous systems. In non-synchronous systems, however, the search for third body periodic orbits is complicated by several factors. The mathematical model for the third-body motion is now time-variant, the motion of P_2 is not trivial and also requires the distinction between P_1- and P_2-fixed rotating frames.

INTRODUCTION

While most of the more massive bodies in the solar system, e.g., the planets and the Sun, are reasonably spherically-shaped, there are many smaller objects with very irregular shapes that orbit the Sun or even a planet. These irregular bodies are the focus of increasing scientific interest and their study, through various types of observations, offers insight into the early development of the solar system, as well as the formation and origin of more massive bodies such as the planets. However, ground-based observations possess limited capabilities and closer observations, available during in situ missions that involve close encounters or sample-return scenarios, supply higher volume and higher quality data for analysis. Yet, to successfully design trajectories to reach such small arbitrarily-shaped bodies and explore the nearby regions, a thorough understanding of the dynamical environment in the vicinity of such systems is required.

In recent years, several spacecraft have been delivered to the vicinity of small irregular bodies and more complex missions are under development. In 2001, after a series of orbital revolutions to bring the NEAR spacecraft closer to the asteroid 433 Eros and to gather more scientific observations, the vehicle landed on the asteroid surface.[1] Launched in 2007, the current Dawn project is another mission to irregular bodies, with a spacecraft that orbited Vesta for over a year and is now enroute to the dwarf planet Ceres.[2] The Russian Phobos-Graunt spacecraft, launched in November 2011, originally planned to land a probe on Phobos and return a soil sample to Earth; unfortunately, the spacecraft never left Earth orbit.[3] In 2016, the NASA mission OSIRIS-REX is scheduled to deliver a spacecraft to the asteroid 1999 RQ36 to collect soil samples and to investigate this potentially

*Ph.D Student, School of Aeronautics and Astronautics, Purdue University, 701 W Stadium Ave., West Lafayette, IN 47906; Member AAS, AIAA.

†Hsu Lo Professor, School of Aeronautics and Astronautics, Purdue University, 701 W Stadium Ave., West Lafayette, IN 47906; Fellow AAS, AIAA.

hazardous object.[4] The number of proposals involving such spacecraft destinations is increasing. Current estimates indicate that approximately sixteen percent of the known near-Earth asteroid population may be binaries[5] and a few new mission concepts are emerging to visit binary systems comprised of irregular bodies. Thus, the dynamical behavior in such an environment requires further investigation. To highlight a longer-term goal, a mission selected for the Assessment Study Phase of the ESA program Cosmic Vision and proposed for a launch between 2020 and 2024, the ESA-led MarcoPolo-R spacecraft is expected to visit a near-Earth binary asteroid.[6] In support of such future endeavors, other authors have investigated the dynamical environment in the vicinity of a pair of irregularly-shaped bodies with a similar ellipsoid-sphere model,[7,8] and some investigations have been completed with alternative approaches that are based on modeling of the primary bodies as a geometric polyhedron.[9,10]

The focus of this investigation is the exploration of trajectories in the vicinity of a system comprised of two bodies, one modeled as a massive ellipsoid and a second massive spherical body. One objective of this analysis is the design of third-body trajectories that exhibit some desired characteristics within the context of exploring the primary bodies or the nearby region. Two primary configurations are addressed: 'synchronous' and 'non-synchronous'. The synchronous configuration is a time-invariant problem, analogous to the Circular Restricted Three Body Problem (CR3BP) regime, that is, the relative positions of the two primaries are straightforward and known over any specified time interval. Thus, concepts and tools similar to those applied in the CR3BP are available to design the third-body trajectories. In non-synchronous systems, however, the motion of the primary system is not trivial and a Full Two-Body Problem (F2BP) is formulated to describe the motion of the sphere P_2 with respect to the ellipsoid P_1. Then, the dynamical model that describes the behavior of a test particle is time-variant and the same tools are not directly applicable. To motivate the introduction of these models, the familiar circular restricted three-body problem applied to systems of small bodies is also discussed.

DYNAMICAL MODELS DEVELOPMENT

Within the context of trajectory exploration of nearby systems comprised of small irregular bodies, a first step in the analysis is to develop a dynamical model that describes the motion of the primary system. Then, to incorporate the motion of a third body, additional dynamical models that describe the third-body behavior for different levels of complexity in the primary system model are constructed.

Full Two-Body Problem (F2BP)

Definition. To describe the mutual motion of a pair of massive bodies, consider the full two-body problem. Define one primary, P_1, as an ellipsoid with semi-major axes α, β, and γ, and let P_2, the second primary, be spherical.[7,8] The distance separating the two primaries is denoted r, and m_1 and m_2 are the individual masses of P_1 and P_2, respectively, with mass ratio $\nu = m_2/(m_1 + m_2)$. Both bodies are uniform with constant density. In general, the motion of P_2, with respect to P_1, is numerically simulated in a rotating frame (R_{P_1}) that is fixed with the ellipsoidal primary P_1 with unit vectors that are aligned in the ellipsoid semi-major axes. A second rotating frame (R_{P_2}), one that is rotating with the second primary, i.e., P_2, is also introduced, as illustrated in Figure 1. While the numerical integration is always accomplished in frame R_{P_1}, the visualization of the integrated trajectory is often more intuitive when viewed from frame R_{P_2}, as the path appears similar to more widely employed trajectory representations.

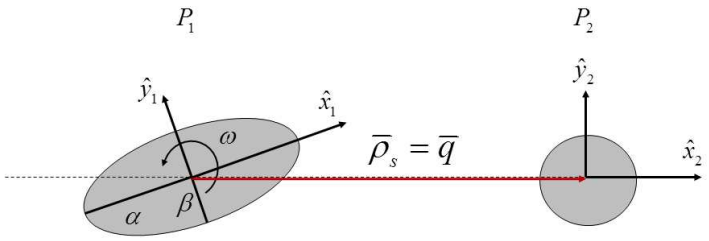

Figure 1. Full Two Body Problem (F2BP) geometry

Equations of the motion. The Equations of Motion (EOM) for the mutual motion of a sphere and an ellipsoid are derived from Newton's second law of motion, as viewed by an inertial observer. To facilitate numerical exploration, a set of characteristic quantities to nondimensionalize the equations are introduced. The characteristic distance is selected as the largest ellipsoid semi-major axes α and the characteristic time is defined as the inverse of the mean orbital motion of the system at this radius, that is, $t^* = \sqrt{\alpha/G(m_1+m_2)}$. In the rotating frame that is fixed with the ellipsoid, the nondimensional translational and rotational equations of motion are written,

$$\ddot{\bar{\rho}}_s + 2\bar{\omega} \times \dot{\bar{\rho}}_s + \bar{\omega} \times (\bar{\omega} \times \bar{\rho}_s) + \dot{\bar{\omega}} \times \bar{\rho}_s = \frac{\partial U_e}{\partial \bar{\rho}_s} \tag{1}$$

$$\bar{\bar{I}} \cdot \dot{\bar{\omega}} + \bar{\omega} \times \bar{\bar{I}} \cdot \bar{\omega} = -\nu \bar{\rho}_s \times \frac{\partial U_e}{\partial \bar{\rho}_s} \tag{2}$$

where $\bar{\rho}_s = x_s\hat{x}_1 + y_s\hat{y}_1 + z_s\hat{z}_1$ is the nondimensional position vector that denotes the location of the center of mass of the spherical primary with respect to the ellipsoid center of mass in the ellipsoid-fixed rotating frame, $\bar{\omega}$ is the angular spin rate of the ellipsoidal primary such that $\bar{\omega}$ is aligned with the inertial $\hat{Z}$ direction, $\bar{\bar{I}}$ is the inertia dyadic for the ellipsoid, and U_e denotes the gravitational potential. Dots denote derivatives with respect to time as viewed by an observer in the working rotating frame, that is, R_{P_1}. It is further assumed that the two primaries move along coplanar orbits, as viewed by an inertial observer, reducing the problem to a two degree-of-freedom Hamiltonian system. In Hamiltonian form, these EOMs are written in the form,

$$\dot{\bar{q}} = H_{\bar{p}} \;\; ; \;\; \dot{\bar{r}} = -H_{\bar{q}} \tag{3}$$

where $\bar{q}$ represents the position vector that denotes the location of the sphere with respect to the ellipsoid in the R_{P_1} frame, $\bar{p}$ denotes the corresponding inertial velocity vector, and H is the scalar Hamiltonian. Formulating the problem in terms of Hamiltonian variables offers the advantage of explicit expressions for the angular rate ω and its rate of change $\dot{\omega}$. The Hamiltonian for the ellipsoid-sphere system is,

$$H = \frac{1}{2}\bar{p}.\bar{p} + \frac{\nu}{2I_{zz}}\left[K - \hat{z} \cdot (\bar{q} \times \bar{p})\right]^2 - U_e \tag{4}$$

where I_{zz} is the ellipsoid moment of inertia along the inertial $\hat{Z}$ direction, K is the magnitude of the angular momentum of the system, and U_e denotes the mutual potential of the ellipsoid-sphere

system, that is, computed as an elliptical integral. These equations of the motion are numerically integrated to simulate the behavior of any given ellipsoid-sphere system.

Synchronous and non-synchronous systems. From the general formulation, two equilibrium primary configurations are identified: the long-axis equilibrium and the short-axis equilibrium configurations. Initially, consider the long-axis configuration, that is, a primary orientation such that the ellipsoid largest semi-major axis direction, α, is aligned with the ellipsoid-sphere direction $\hat{x}_2$. For this configuration to be maintained, both rotating frames coincide and the primaries P_1 and P_2 appear to be fixed in the rotating frame. This configuration is labeled 'synchronous'. The primaries may also move in a configuration that is not fixed relative to an inertial observer. For 'non-synchronous' systems, the spin rate of P_1 and the orbital rate of P_2 differ as viewed from the inertial frame.

Three-body Dynamical Models

General formulation: non-synchronous systems. The motion of a massless third-body is modeled assuming that the primary system is comprised of the two massive bodies, P_1 and P_2, as illustrated in Figure 2. Note in the figure that the third particle is located relative to the ellipsoid center of mass, as viewed in the ellipsoid-fixed frame, by the position vector $\bar{\rho}_e = x_e\hat{x}_1 + y_e\hat{y}_1 + z_e\hat{z}_1$. Similar to the full two-body problem, the equations of the motion that describe the behavior of a massless particle near a primary system are derived from Newton's second law, that is, the acceleration of a particle in the gravity field is derived from the gradient of the gravitational potential function. The EOMs are,

$$\ddot{\bar{\rho}}_e + 2\bar{\omega} \times \dot{\bar{\rho}}_e + \bar{\omega} \times (\bar{\omega} \times \bar{\rho}_e) + \dot{\bar{\omega}} \times \bar{\rho}_e = \frac{\partial U}{\partial \bar{\rho}_e} + \frac{\partial U_e}{\partial \bar{q}} \tag{5}$$

where $\bar{q}$ represents the location of the sphere center of mass and $\bar{\omega}$ is the orbital angular rate of the ellipsoidal primary P_1. The symbol U then denotes the gravitational potential defined as $U = \nu U_s + (1-\nu)U_e$ where U_s and U_e represent the potential that is associated with the sphere and the ellipsoid, respectively. Since no analytical solution to the EOMs exists, the set of differential equations is numerically integrated along with the F2BP EOMs to simulate the motion of a massless third particle.

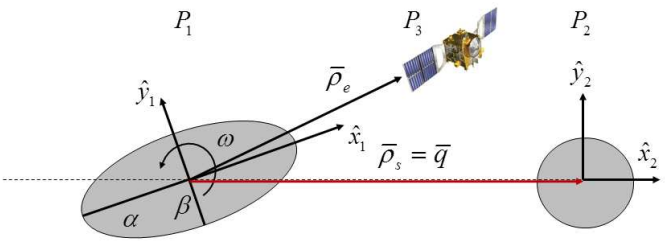

Figure 2. Three-body problem geometry under periodic F2BP

Synchronous sphere-ellipsoid systems. The complex dynamical model is initially assumed to be based on a synchronous system, i.e., the behavior of a third body is sought in the vicinity of a synchronous sphere-ellipsoid binary system. Thus, a three-body problem is constructed assuming that

the position of both primaries remains fixed with respect to the R_{P1} rotating frame. For this simplified problem, both rotating frames, labeled R_{P_1} and R_{P_2}, coincide through any time evolution; thus, for clarity, a unique rotating frame is centered at the system barycenter, as illustrated in Figure 3. Note that the directions of the unit vectors for R_{P_1} and R_{P_2}, as well as the barycentered system in Figure 3, all coincide. Such a system is a reduction of the more general problem as formulated for non-synchronous systems, and the vector EOM is similar but distinguished by the disappearance of the term $\frac{\partial U_e}{\partial \bar{q}}$. Also true in synchronous systems, the angular velocity $\bar{\omega}$ is constant in both magnitude and direction and the EOM reduces to the scalar form,

$$\ddot{x} - 2\omega\dot{y} = U_x^* \; ; \; \ddot{y} + 2\omega\dot{x} = U_y^* \; ; \; \ddot{z} = U_z^* \tag{6}$$

where $\bar{\rho} = x\hat{x} + y\hat{y} + z\hat{z}$ now represents the location of the third body with respect to the system barycenter, $\bar{\omega}$ is the orbital angular velocity of the system and U_i^* are the first partial derivatives of the pseudo-potential with respect to the position vector, defined as $U^* = U + \frac{1}{2}\omega^2(x^2 + y^2)$. Note that this set of scalar equations is time-invariant; however, no analytical solution to the EOMs exists and the set of differential equations is numerically integrated to simulate the motion of the massless particle.

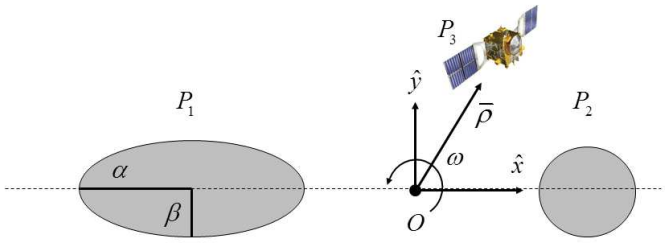

Figure 3. Three-body problem geometry under synchronous F2BP

Point mass systems. A further reduction in the complexity of the model is a primary system that is comprised of two spherical bodies rather than ellipsoidal and spherical primaries, that is, the circular restricted three-body problem. In the CR3BP, the motion of a massless third body is modeled assuming that the primary system is comprised of two point mass bodies. It is further assumed that the two primaries move along coplanar circular orbits, as viewed by an inertial observer. Because the CR3BP is employed in a variety of different problems, including the modeling of planetary systems, the characteristic distance is generally selected as the separation between the primaries and the characteristic time now corresponds to the period of the primary system. Thus, the equations of motion are similar to the synchronous sphere-ellipsoid systems, that is,

$$\ddot{x} - 2n\dot{y} = U_x^* \; ; \; \ddot{y} + 2n\dot{x} = U_y^* \; ; \; \ddot{z} = U_z^* \tag{7}$$

where U_i^* are the first derivatives of the pseudo-potential defined as $U^* = U + \frac{1}{2}n^2(x^2 + y^2)$ and $n = 1$ is the nondimensional mean motion of the primary system. Similar to the differential equations governing the behavior in synchronous systems, although the scalar relationships in Eq. (7) are time-invariant, the set of differential equations does not admit any analytical solution and numerical exploration is required to simulate the motion of a massless particle.

CIRCULAR RESTRICTED THREE-BODY PROBLEM (CR3BP): BINARY SYSTEM

Before focusing on trajectory exploration within systems with added complexity in the dynamical models that describe the motion of the binary (primary) system of interest, first consider the more familiar CR3BP. The focus of this investigation is on systems of small bodies, with application to binary asteroid systems; thus, systems with large value of the mass ratio ν, e.g., 0.1 to 0.3, are of particular interest.

Equilibrium Solutions, Jacobi Constant, and Zero Velocity Curves (ZVC)

In general, the equations of the motion, as formulated in the rotating frame, admit five equilibrium solutions that manifest as five equilibrium locations where the motion of a test particle remains stationary over any time evolution. The equilibrium locations for a sample system with mass ratio $\nu = 0.3$ in the CR3BP are illustrated in Figure 4. Note that there are three collinear points, labeled

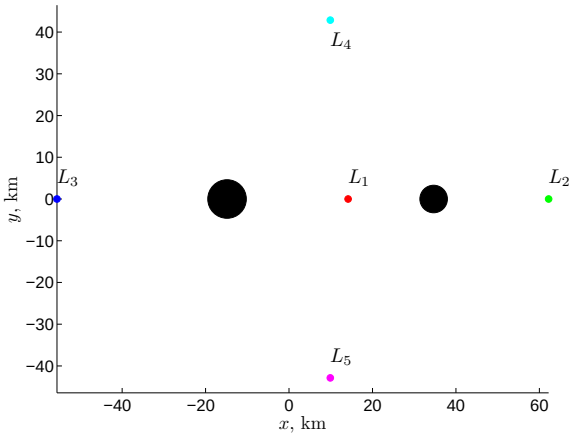

Figure 4. Lagrange points in the CR3BP - $\nu = 0.3$

L_1, L_2, L_3 and two equilateral points L_4 and L_5. The equations of motion expressed in terms of the pseudo-potential function, with respect to the rotating frame, also allow the existence of a unique integral of the motion, i.e., the Jacobi integral, i.e.,

$$C = 2U^* - \frac{1}{2}(\dot{x}^2 + \dot{y}^2 + \dot{z}^2) \tag{8}$$

The equilibrium solutions and the Jacobi constant are the basis of another important concept. While no analytical solution exists to describe the motion of a particle within this dynamical environment, the motion is bounded under certain conditions. In this dynamical regime, the boundedness of the motion for a specific energy level, or Jacobi constant, is represented by the Zero Velocity Curves (ZVC) that decompose the space in the vicinity of the two primaries into regions where the motion is possible and regions where the motion is not physically allowable. In Figure 5, ZVCs for representative Jacobi constant values are plotted for a system with mass ratio equal to 0.3. The color scale in Figure 5 represents the nondimensional Jacobi constant value that is associated with each curve. For decreasing Jacobi values, or increasing energy levels, ZVCs that originally encompass both primaries evolve: the curves merge at the collinear points, first, to open up gateways in the $x-y$ plane for the motion of a third body. Eventually, any constraint on the motion of a test particle is cleared.

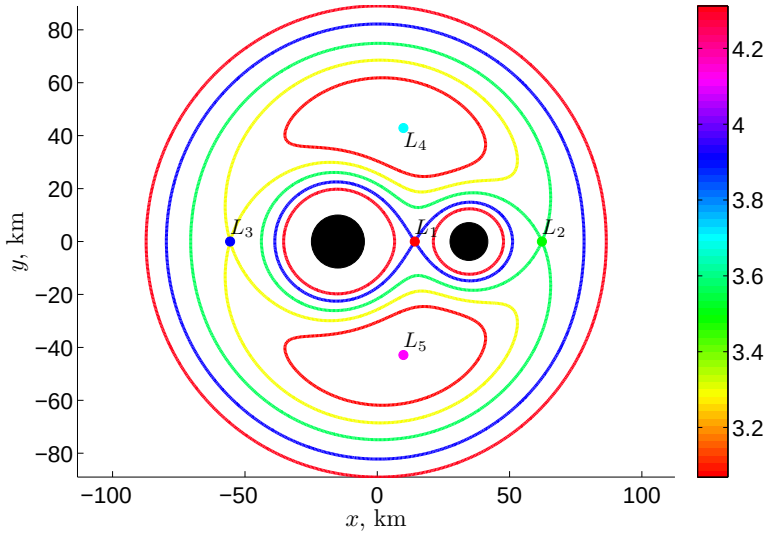

Figure 5. ZVCs in the CR3BP for representative Jacobi constant values - $\nu = 0.3$

Periodic Orbits in the CR3BP

To explore the dynamical behavior of a third body in the vicinity of two spherical primaries, periodic orbits are of special interest. A differential-corrector based technique is employed to compute a trajectory that is periodic in the nonlinear regime given some initial guess. Most common families of periodic orbits within this regime are labeled libration point orbits and the first-order variational equations of the motion are employed to generate an initial guess in the vicinity of a given equilibrium point. Planar Lyapunov families of periodic orbits associated with different collinear equilibrium points appear in Figure 6; other families of three-dimensional orbits can also be computed.[11]

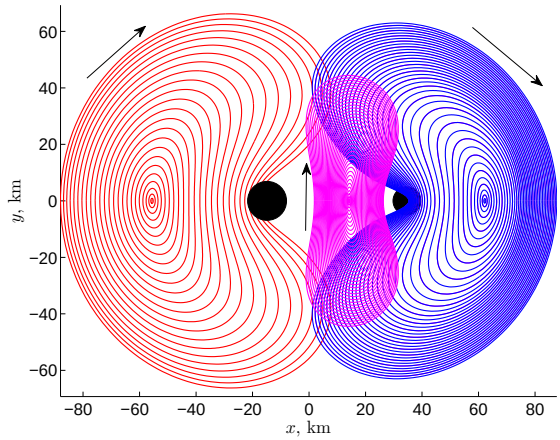

Figure 6. L_1**,** L_2**, and**L_3 **Lyapunov families in the CR3BP for mass ratio** $\nu = 0.3$

THREE-BODY PROBLEM: SYNCHRONOUS FULL TWO-BODY PROBLEM

Within the context of exploring third-body trajectories in the vicinity of two small irregular bodies, that is, a problem where investigating the motion in close proximity of the primaries is necessary, two spherical primaries may not, in general, be a reasonable assumption. This more specific problem motivates the introduction of a dynamical model that incorporates more complexity in the primary system model. As a first step, consider the Synchronous Sphere-Ellipsoid Three-Body Problem (SSETBP). With similar equations of motion, the SSETBP possesses attributes similar to those in the CR3BP. In particular, while no analytical solution for the motion of the particle is available, other concepts, such as equilibrium solutions, integrals of the motion and zero velocity curves, are insightful.

Equivalent Lagrange Points

Similar to the CR3BP, the EOMs admit, in general, five equilibrium solutions that satisfy the vector equation $\partial U/\partial \bar{\rho} = \bar{0}$. Because of the symmetry properties of the primaries, note that the equilibrium solutions occur in locations that mimic the general equilibrium positions in the CR3BP: 3 collinear points and 2 equilateral points, labeled as equivalent Lagrange points. The correlation between the CR3BP and the new problem is highlighted by computing the equilibrium solutions for an array of sphere-ellipsoid systems. From a system that is equivalent to the CR3BP regime, that is, an ellipsoid primary with semi-major axes $\alpha = \beta = \gamma = 1$, continuing semi-major axes parameters β and γ from 1 to 0.5, that is, from the initial sphere-sphere system toward an ellipsoid-sphere system with a very elongated primary, the corresponding equilibrium locations for each system are straightforwardly constructed. In Figure 7, the locations of the equilibrium positions are illustrated

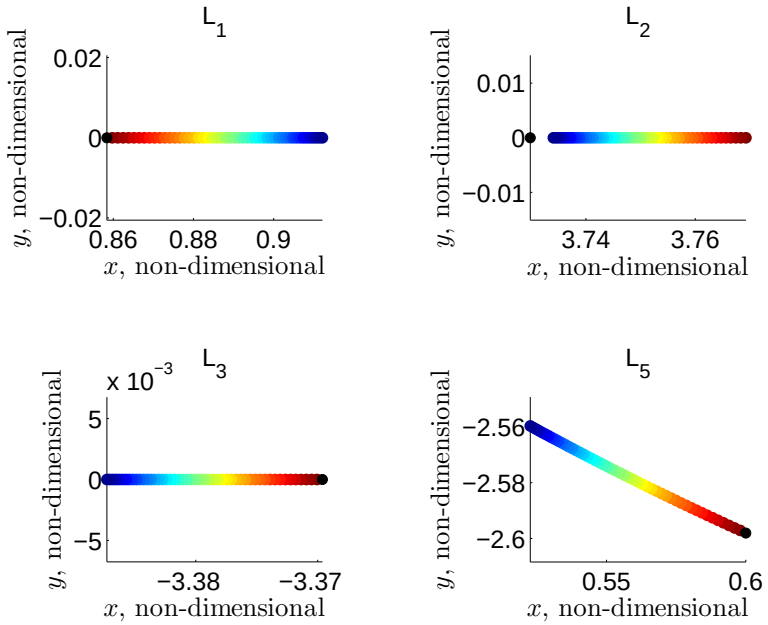

Figure 7. Continuation of equivalent Lagrange points from $\beta = \gamma = 1$ to $\beta = \gamma = 0.5$ - $\nu = 0.3$ - $r = 3$

for systems with mass ratio $\nu = 0.3$ for the points L_1, L_2, L_3, and L_4 (L_5 is the mirror of L_4 across the x axis); the color scale, from blue to red, represents a decreasing value of the ellipsoid semi-

major axes β and γ from 1 to 0.5 such that $\alpha = 1$ and $\beta = \gamma$. Note that as the ellipsoid primary becomes more elongated, from the initial sphere-sphere system, the locations of the equilibrium solutions migrate accordingly. The points L_1 and L_3 tend to shift toward P_1 while L_2 is migrating away from both primaries. Also, L_4 and L_5 move laterally toward the primaries, that is, along the y-axis direction, and migrate axially, that is, along the x-axis direction, toward P_2.

Zero velocity Curves for a Synchronous Ellipsoid - Sphere System.

Similar to the CR3BP, the EOMs relative to the ellipsoid-fixed rotating frame admits one integral of the motion with an expression that is equivalent to the expression for the Jacobi constant in the CR3BP as given in Eq. (8). Thus, when considering an ellipsoidal primary, the motion of a third body remains bounded depending on the energy level, that is, for a given value of the Jacobi constant, and for certain specified conditions. The evolution of the ZVCs is generally similar to the CR3BP for any given ellipsoid-sphere system; the curves are, however, shaped differently to reflect the non-spherical shape of P_1.

STRATEGY TO COMPUTE PERIODIC ORBITS IN SYNCHRONOUS SYSTEMS

Libration Point Periodic Orbits

Families of periodic orbits are computed for a sphere-ellipsoid system that are similar to the well-known CR3BP families of libration point periodic orbits, that is, families of trajectories that originate in the vicinity of a particular equilibrium point. Recall that the motion of the sphere relative to the fixed ellipsoid is consistent with the full two-body problem, that is, for synchronous systems the two primaries are fixed as viewed in the rotating frame. First, the planar Lyapunov families corresponding to the equivalent collinear Lagrange points are computed for a sample ellipsoid-sphere system with an elongated primary. Employing a continuation strategy, additional families of more complex orbits that include three-dimensional trajectories are also computed, as illustrated in Figure 8. In this plot are displayed Lyapunov, halo, and axial families of periodic orbits associated with each of the collinear points. Although not illustrated in this figure, similar families of orbits can also be constructed in the vicinity of the equilateral points. Although these families of orbits may or may not offer options for any direct application in design or analysis scenarios, these trajectories are most useful in constructing even more complex orbits.

Heteroclinic and Homoclinic Cycles

Exploiting the tools available from the analysis in the CR3BP, trajectories for a third body in close proximity to the primaries in synchronous systems are designed. Within the context of trajectory exploration for application to binary systems of asteroids, the focus in this investigation is on the construction of trajectories that exhibit a specific behavior, that is, periodic trajectories that shift back and forth between the regions dominated by each of the equivalent collinear libration points, as viewed in the rotating frame, offering repeated close passages of both primaries. A strategy similar to the computation of homoclinic and heteroclinic connections in the CR3BP is employed.[12,13] The steps in a process to compute periodic trajectories include: (i) computation of a suite of families of periodic libration point orbits for a given system; (ii) determination and computation of the associated manifolds corresponding to one libration point family at a desired energy level, i.e., a fixed Jacobi constant value; (iii) selection of specific manifold arcs and subsequent construction of an initial guess for a periodic path linking arcs in the vicinity of one or several libration points;

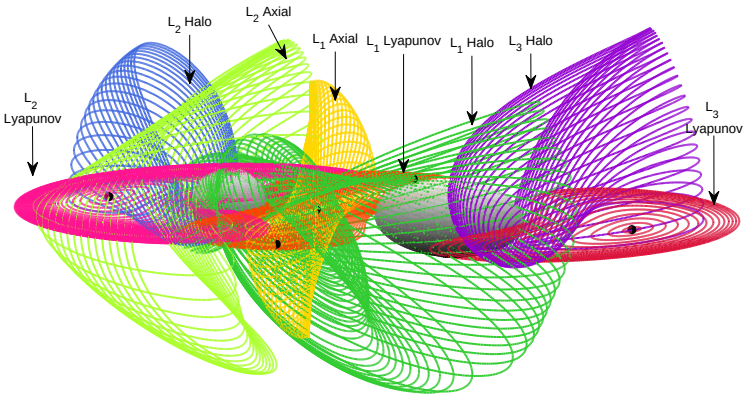

Figure 8. Libration point Periodic Orbits (LPO): ellipsoid axes ratios $\beta = \gamma = 0.5$ - primary mass ratio $\nu = 0.3$ - primary distance $r = 3$

and, (iv) insertion of the initial guess into a prediction-correction algorithm to produce one or more periodic trajectories that retain the desired characteristics.

Homoclinic cycles. Within the framework of the CR3BP, a closed trajectory that connects a periodic orbit with itself, that is, an arc that departs and returns to the same periodic orbit, is labeled a homoclinic connection. The construction of such a trajectory is often achieved by exploiting the unstable and stable manifold arcs that are associated with the periodic orbit of interest to produce an initial guess. Within the context of trajectory exploration within binary systems of small bodies, consider a scenario that involves periodic trajectories that shift back and forth between the libration points L_1, L_2 and L_3, as viewed in the rotating frame. An initial guess for such a trajectory is constructed from a double homoclinic connection for a periodic L_1 libration point orbit, that is, assembling two independent connections from the L_1 orbit, one that extends toward the L_3 point and the second that visits the vicinity of the L_2 point. This process is realized by selecting unstable and stable manifolds arcs that are associated with a L_1 Lyapunov periodic orbit. In Figure 9 are illustrated the unstable and stable manifold tubes for a L_1 Lyapunov orbit in a sphere-ellipsoid system with mass ratio $\nu = 0.3$, primary separation $r = 3$ and semi-major axes $\beta = \gamma = 0.5$. The corresponding manifold tubes extend toward both P_1 and P_2, visiting the vicinity of two other libration points, that is, L_3 and L_2, respectively. To facilitate the selection of suitable manifolds arcs, a Poincaré section is employed. In this planar analysis, each manifold tube is numerically propagated until the first intersection with a specified hyperplane, specifically, $y = 0$, as defined in the rotating frame. The end result is a trajectory that is continuous both in position and velocity at the originating periodic orbit and at the hyperplane intersection. Considering planar trajectories, the hyperplane reduces the dimensionality of the problem to three variables. In addition, recall the existence of one integral the motion, the Jacobi constant, that further reduces the problem to two dimensions. One possible representation for the selection of a suitable set of manifold arcs is a Poincaré map $x - \dot{x}$ of the first crossings of the manifold tube with the hyperplane. The manifolds associated with an L_1 Lyapunov orbit at a specified energy level are plotted in Figure 9 in configuration space. The Poincaré map that corresponds to the crossings of the manifolds with the hyperplane $y = 0$ are illustrated in Figure 10. The upper plot represents the crossings with negative x coordinates that correspond to crossings with the hyperplane to the left of P_1; the bottom plot

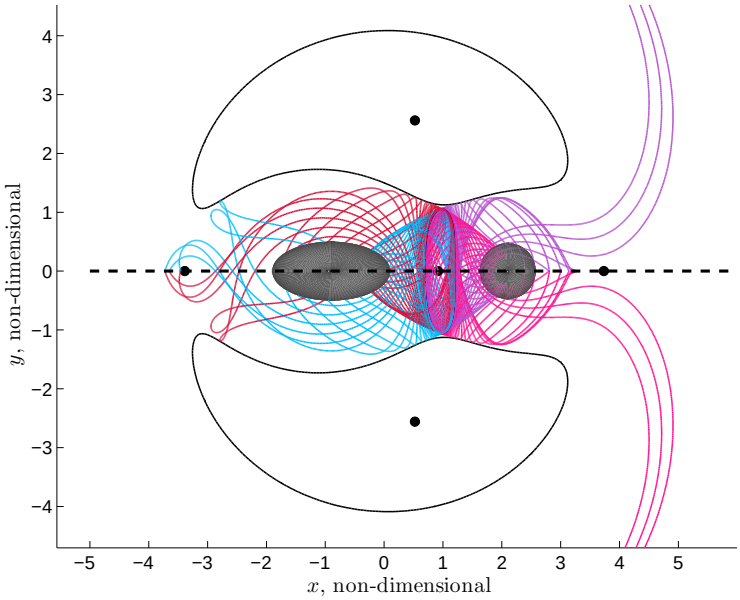

Figure 9. Unstable and stable manifold arcs for L_1 Lyapunov orbit for $\beta = \gamma = 0.5 - \nu = 0.3 - r = 3$

depicts the crossings that occur on the right side of P_2. Red and magenta dots denote crossings of the unstable manifold arcs, blue and purple dots correspond to stable manifold arc crossings. An initial guess for a periodic orbit is constructed from the selection of two manifold arcs, one stable and one unstable, that pass through the vicinity of the L_3 point and two arcs that extend toward L_2. On the Poincaré map representation, the objective is the selection of two points on each map (both the top and the bottom plot), one that corresponds to a stable manifold arc and the second to an unstable arc, that intersect both in position and velocity, that is, in terms of the coordinates x and $\dot{x}$. If no intersection is apparent, points with the smallest separation on the map are the most suitable candidates to produce a reasonable initial guess. Because of the symmetry properties of the problem, manifold arcs that cross the hyperplane with the smallest transversal velocity $\dot{x}$ often yield a satisfactory initial guess. A differential corrections algorithm is employed to produce a periodic trajectory that retains the desired characteristics present in the initial guess. Further, a continuation method allows the generation of a family of similar trajectories. A set of trajectories that result from this design process appears in Figure 11. The family of planar periodic trajectories includes members that all shift back and forth between the libration points L_1, L_2 and L_3, as displayed in the rotating frame.

Heteroclinic cycles. Another useful concept in the design of trajectories that exhibit behavior similar to the periodic orbits produced exploiting homoclinic connections, that is, trajectories that shift back and forth between the libration points L_1, L_2 and L_3 is often labeled a heteroclinic connection, that is, a trajectory arc that naturally links two periodic orbits with no position or velocity discontinuity. The process to construct an initial guess for such a heteroclinic connection is similar to the strategy to produce homoclinic connections but involves two distinct periodic orbits. Often, manifold arcs that are associated with both periodic orbits, stable and unstable, are computed and exploited to determine an initial guess for the desired connection. To design a periodic trajectory

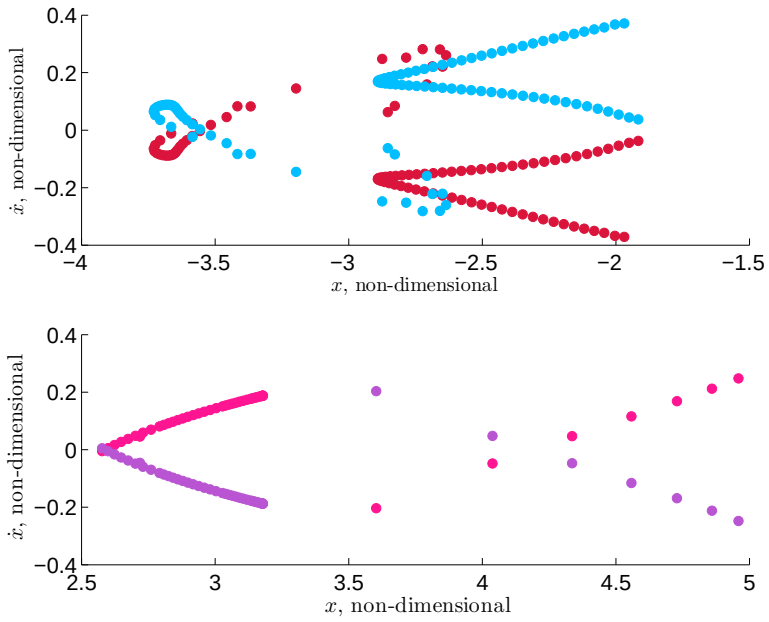

Figure 10. Unstable and stable manifold arc crossings for L_1 Lyapunov orbit for $\beta = \gamma = 0.5 - \nu = 0.3 - r = 3$

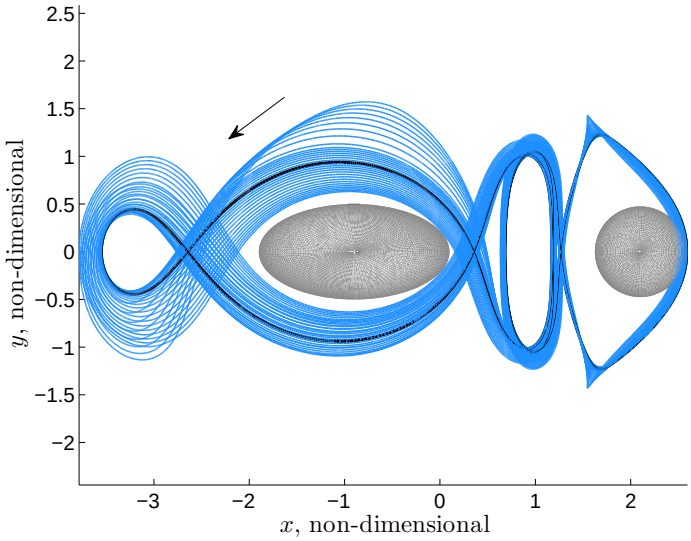

Figure 11. Family of double homoclinic periodic cycles for $\beta = \gamma = 0.5 - \nu = 0.3 - r = 3$

that visits the vicinity of all three collinear libration points, consider an initial guess that is constructed from a double heteroclinic cycle, that is, an initially discontinuous path that is formed from two independent heteroclinic connections. Consider three libration point periodic orbits with similar Jacobi constant values that are centered around L_1, L_2, and L_3, respectively. Then, a double cycle is then constructed from two heteroclinic connections, one between the L_1 and L_3 orbits and the second between the L_1 and L_2 orbits. The initial guess process is initiated via unstable and stable manifold arcs that are associated with a L_1 and L_3 Lyapunov orbits at the same energy level, i.e., same value of Jacobi constant, respectively. A second arc is comprised of stable and unstable manifold arcs from the same L_1 trajectory and an L_2 Lyapunov orbit, as illustrated in Figure 12. Similar to a homoclinic cycle, a Poincaré section approach is developed to aid the selection of

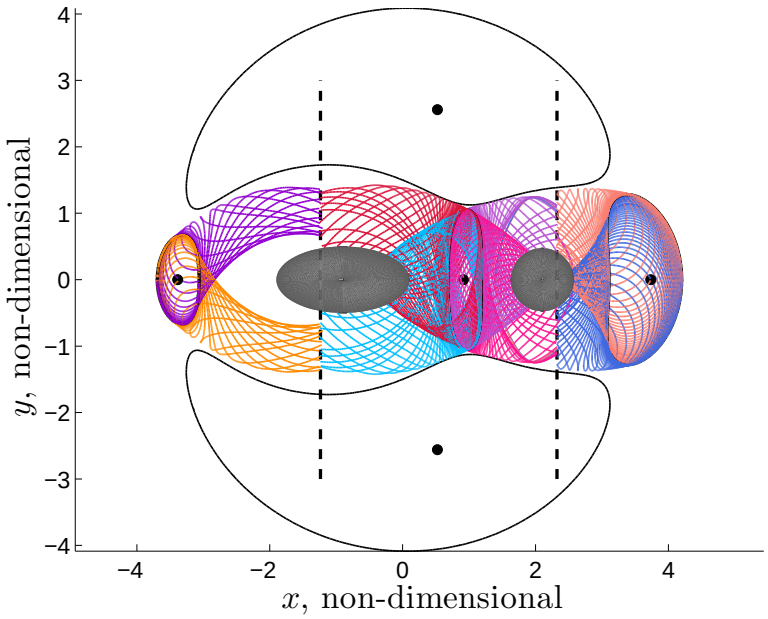

Figure 12. Unstable and stable manifold arcs for L_1, L_2, and L_3 Lyapunov orbit for $\beta = \gamma = 0.5 - \nu = 0.3 - r = 3$

suitable manifold arcs. Consider two hyperplanes, one defined as $x = 1/2(x_{L_1} + x_{L_3})$ where x_{L_1} and x_{L_3} denote the locations of the L_1 and L_3 libration points, and a second hyperplane such that $x = 1/2(x_{L_1} + x_{L_2})$. The process to generate the initial guess is illustrated in Figure 12. Unstable and stable manifold arcs computed for the selected L_1, L_2, and L_3 Lyapunov orbits are displayed in the figure until the first intersection with the corresponding hyperplane. Also, similar to the approach for homoclinic connections, the crossings of the manifold arcs with the hyperplane for both unstable and stable manifolds are represented on a $y - \dot{y}$ Poincaré map. From this representation, the selection process for the manifold arcs that are used to construct the initial guess is guided by the same principles, that is, unstable and stable points on the map that intersect or nearly intersect are employed to create a reasonable, possibly discontinuous, trajectory. The complete initial guess is corrected to produce a periodic orbit that retains the desired characteristics. The orbit obtained from the correction process is subsequently exploited to initialize a continuation method to generate a family of similar periodic trajectories, as illustrated in Figure 13.

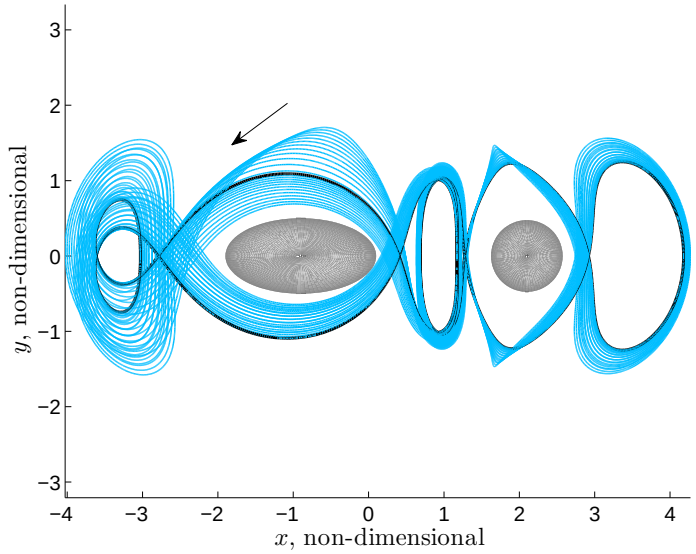

Figure 13. Family of double heteroclinic periodic cycles for $\beta = \gamma = 0.5 - \nu = 0.3 - r = 3$

THREE-BODY PROBLEM: NON-SYNCHRONOUS FULL TWO-BODY PROBLEM

Non-Synchronous Systems

While synchronous systems, or close-to-synchronous systems, are available in the known asteroid population, systems also exist where the primaries move in a configuration that is not fixed relative to the rotating frame. For 'non-synchronous' systems, the spin rate of ellipsoidal body P_1 and the orbital rate of P_2 are different as viewed from the inertial frame. The initial challenge then is the motion of the two-body system. Given various possible approaches to this problem, initially consider an analogy with a simple problem, the simple pendulum. The motion of a simple pendulum is described by a simple scalar equation in terms of one time-dependent angular coordinate, θ, that is measured relative to the stable equilibrium orientation. The geometry of the problem is illustrated in Figure 14(a) and the EOM is written $\ddot{\theta} + \frac{g}{l} sin\theta = 0$, where g is the constant gravity acceleration and l is the length of the pendulum. Depending on the initial conditions, i.e., θ_0 and $\dot{\theta}_0$, different behavior for the motion of the pendulum is observed and a classic representation that clearly highlights the various types of behavior is a phase space portrait, that is, a θ-$\dot{\theta}$ plot, as illustrated in Figure 14(b). In the figure, are labelled different behaviors that correspond to different characteristic curves in the phase portrait. The fixed points correspond to the equilibrium positions, both stable and unstable. Then, the libration-type behavior is depicted by a set of closed curves centered on a stable equilibrium position. For an alternative set of initial conditions that correspond to increasing total energy, a critical curve exists that divides the phase space into libration (blue) and circulation (red) regions. The boundary is represented by the magenta curve (separatrix) in the phase portrait. This analysis is extended to the problem of interest, that is, the motion of a sphere moving relative to a fixed ellipsoidal body. To exploit the pendulum analogy, define the coordinate θ as the angle between the P_1-P_2 line that corresponds to the equilibrium system, or synchronous system, that is, the x-axis, and the time-dependent location of P_2. A sample path for P_2 is represented, along with the geometry of the problem, in Figure 15 where the trajectory

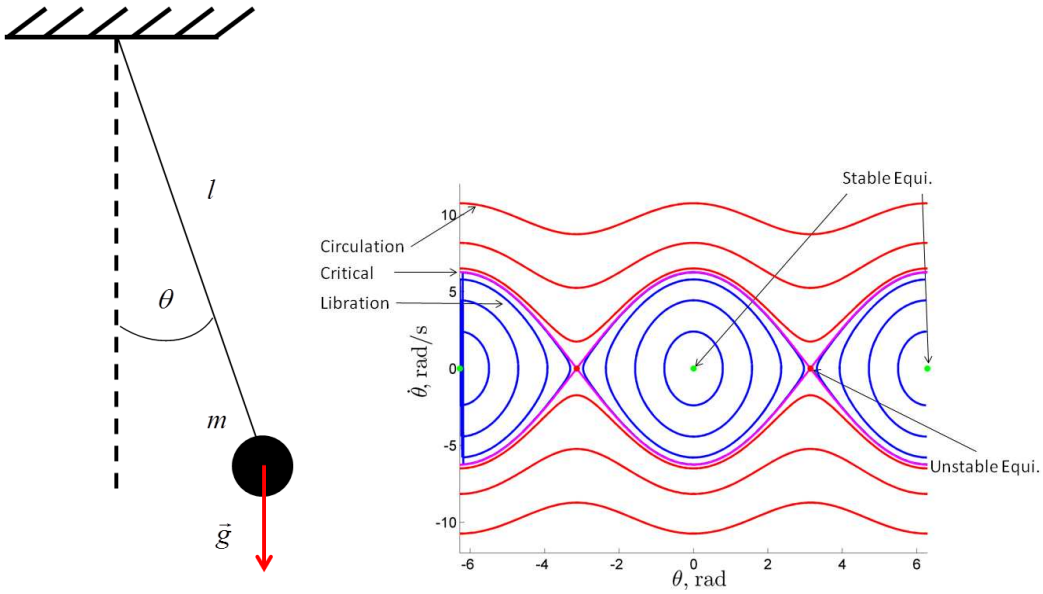

(a) Geometry (b) Simple pendulum phase portrait

Figure 14. Simple pendulum

for the sphere is obtained by perturbing the equilibrium initial conditions. To ensure that the path emerging for P_2 exhibits regular behavior for an extensive time duration, only trajectories that are successfully corrected to periodicity are retained. A set of periodic trajectories for P_2 is generated

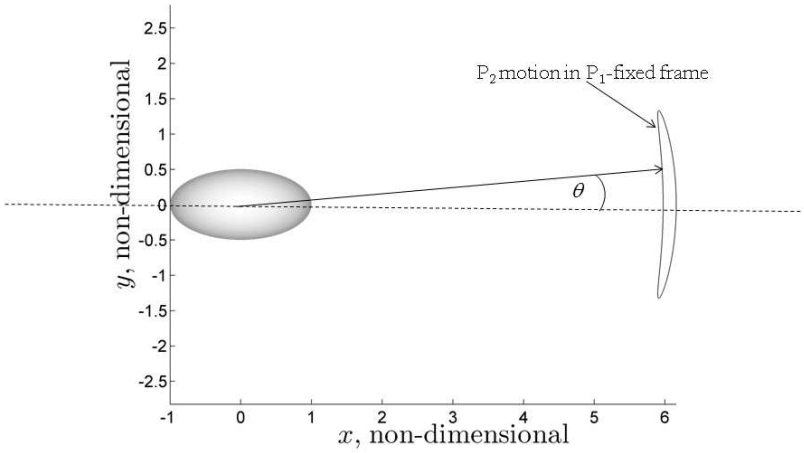

Figure 15. Non-synchronous full two-body problem geometry

from the reference equilibrium configuration varying initial conditions such that the total energy of the system increases. The reference configuration corresponds to a librational motion and the periodic family evolves until the behavior becomes circulatory, as illustrated in Figure 16(a). Similar to the pendulum analysis, the phase portrait that corresponds to the resulting set of trajectories is produced in Figure 16(b) and exhibits the expected characteristics. For further analysis, when incorporating a third body into this dynamical model, the focus is the circulatory behavior. A lower

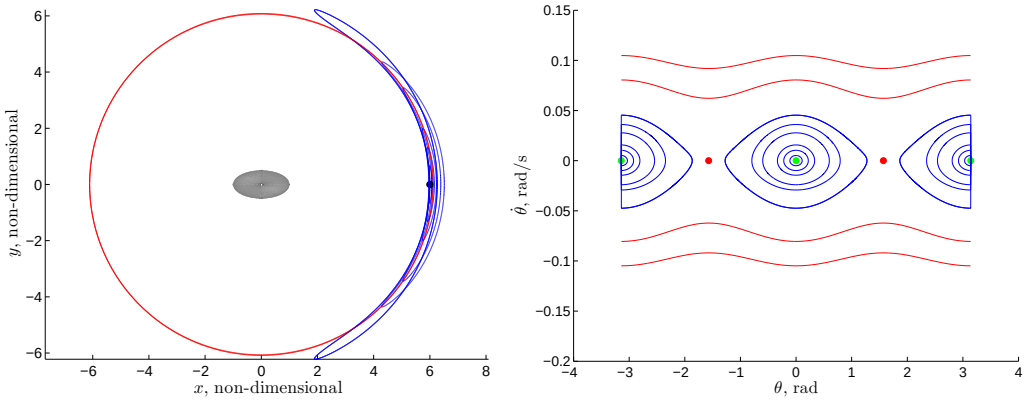

(a) Sample P_2 periodic paths (b) Phase portrait

Figure 16. Non-synchronous full two-body problem

bound is selected for the ratio of the inertial angular velocity rates between P_1 and P_2, that is, the ratio is always greater than two. For the circulation-type motion, the periodic path for P_2 resembles a pseudo-circular orbit, as viewed in the ellipsoid-fixed frame.

Dynamical Substitutes

With a time-dependent solution for the motion of P_2 with respect to P_1, equilibrium solutions to the 3BP EOMs, in the form of fixed stationary points, no longer exist. However, as the path of P_2 is constrained to be periodic, dynamical substitutes that form closed periodic path replace the equivalent Lagrange points from the synchronous case.[14, 15, 16] For any given non-synchronous system, the equivalent Lagrange points for the corresponding synchronous system are employed as initial guesses to compute the dynamical substitutes for the non-synchronous system of interest. In Figure 17, a set of non-synchronous systems that correspond to libration and circulation motions for P_2 are represented as well as the corresponding dynamical substitutes for the equivalent collinear Lagrange points. The upper left view corresponds to the periodic substitutes as viewed in the ellipsoid-fixed frame R_{P_1} and the three collinear dynamical substitutes as viewed in the sphere-fixed frame R_{P_2} are individually illustrated in the three other views. Note that for the computation of the dynamical substitutes, the initial guess for each point is transformed from the R_{P_2} frame to the R_{P_1} frame before the periodic path is computed with a differential corrections algorithm.

Trajectory Exploration in Non-Synchronous Systems

Strategy. A strategy is proposed to construct trajectories that exhibit some set of desired characteristics within the context of the non-synchronous 3BP. The strategy relies on exploiting the insight gained from analysis in the synchronous problem. A first step is the generation of orbits that are periodic in the non-synchronous problem; periodic libration point orbits previously computed from an equivalent synchronous problem are employed as an initial guess. Recall that, in this analysis, the trajectory for P_2 is periodic, thus, for a P_3 periodic trajectory to exist, the period of the desired P_3 orbit must be commensurate with the period of P_2. Consequently, while there exists an infinite set of periodic orbits in the vicinity of a known orbit or a family of orbits in the synchronous case, periodic orbits in the non-synchronous problem are isolated based upon the possible integer ratios

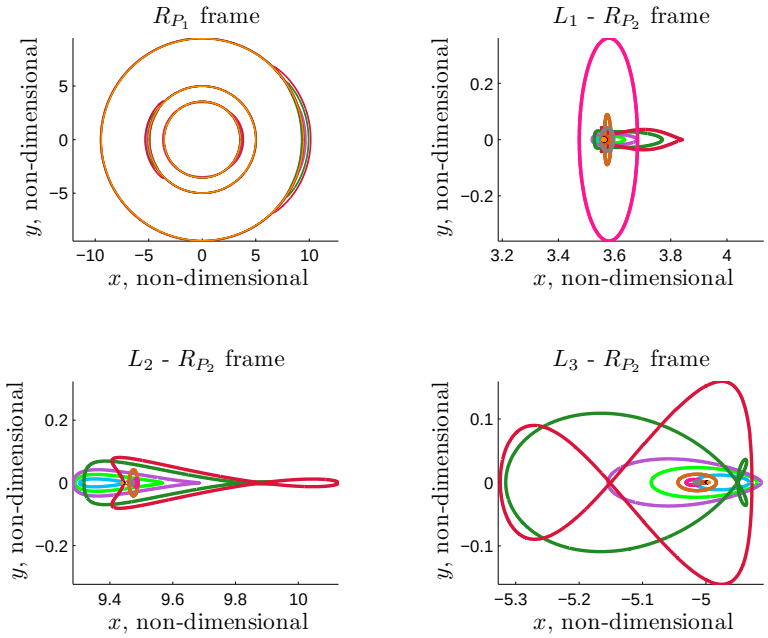

Figure 17. Dynamical substitutes for the equivalent collinear Lagrange points

between the periods of P_3 and P_2. In summary, for any given non-synchronous system, a discrete set of periodic orbits that are equivalent to Lyapunov, halo, axial and vertical synchronous orbits can be computed using the equivalent families of trajectories in the synchronous problem as initial guesses. Note that an initial guess from the synchronous problem is more closely related to a trajectory in the R_{P_2} frame, that is, a frame where the location of the primaries remains almost fixed, that is, only the relative orientation of the primaries significantly changes over time. This initial guess is transformed from the R_{P_2} frame into the R_{P_1} frame prior to any corrections process in the non-synchronous regime. Similar to the analysis in the synchronous problem, a discrete set of isolated libration point orbits is likely not directly relevant for any practical application. However, these types of paths serve as a basis for the construction of more complex trajectories that retain some desired characteristics. In fact, the same procedure that is developed within the context of the synchronous problem is adjusted to construct trajectories that visit the regions of the dynamical substitutes for the equivalent collinear Lagrange points as viewed in the P_2-fixed frame. Because the problem is now time-variant, time continuity must also be maintained between trajectory arcs that are employed to construct a fully continuous orbit. Two different procedures for trajectory design are available for application in the synchronous case, one based on a double homoclinic cycle and an alternative strategy that relies on a double heteroclinic cycle. Both approaches are directly translated to the non-synchronous problem analysis.

Application. Consider a sample non-synchronous system with a primary non-dimenional separation $r = 6$ such that the P_2 motion corresponds to circulation-type behavior, that is, in the ellipsoid-fixed frame the trajectory of P_2 resembles a pseudo-circular orbit and P_2 remains almost stationary in the sphere-fixed frame. In Figure 18(a), represented in black, a non-synchronous periodic orbit is plotted, as viewed in the sphere-fixed frame; this orbit is computed from an L_1 Lyapunov orbit for the equivalent synchronous system. The stable and unstable manifolds that correspond to this periodic orbit are also computed. In Figure 18(a), the sample unstable arcs also ap-

pear. These arcs are those that exhibit a behavior of interest for the construction of an initial guess, similar to the synchronous case, to a path that progresses back and forth between the regions of the dynamical substitutes representing the equilibrium points, as viewed in the sphere-fixed frame. Then, consistent with the procedure for the design of double homoclinic cycles, a x-$\dot{x}$ Poincaré map with hyperplane $y = 0$ aids the selection of suitable arcs to construct a reasonable initial guess, as illustrated in Figure 18(b) where the left and right plot correspond to crossings near P_1 and P_2, respectively. Note that, because the manifold arcs are not time-invariant in the non-synchronous problem, the epoch corresponding to the endpoints along the different arcs that are concatenated to produce the initial guess must be very close to equal. This additional dimension is also represented on the Poincaré map by the color of the points that denote each crossing, in terms of the corresponding epoch of P_2 in its periodic orbit. Once the initial guess is constructed, a differential

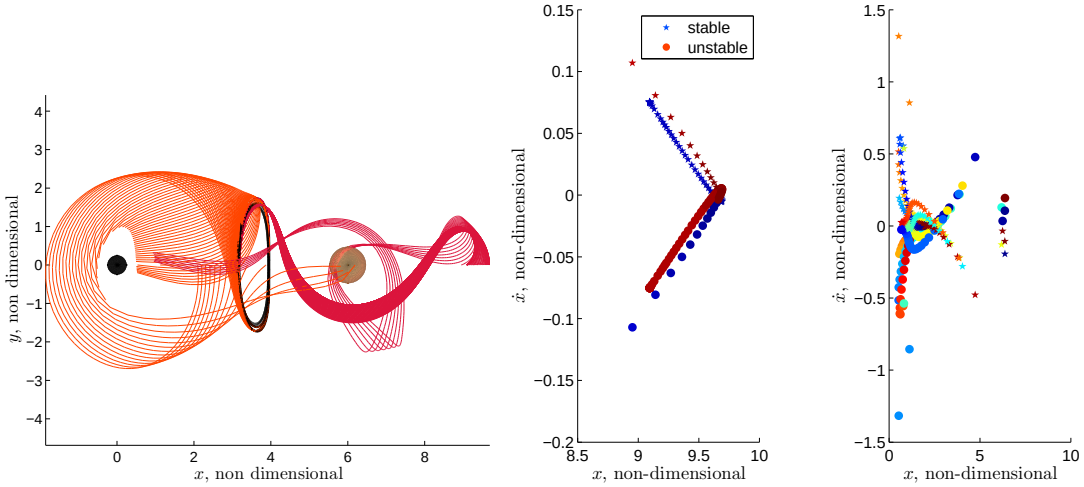

(a) NS Lyapunov orbit manifold arcs - R_{P_2} frame

(b) Poincaré Map x-$\dot{x}$

Figure 18. Strategy for non-synchronous trajectory exploration

corrector is employed to produce a trajectory that retains the desired characteristics. Ideally, such a trajectory is also periodic. However, similar to the results for the non-synchronous periodic orbit, for the designed trajectory to be periodic, the period must be commensurate with the period of P_2. In Figure 19, the result of such a process is plotted, that is, a trajectory that visits the vicinity of all three collinear dynamical substitutes, as viewed in the ellipsoid- and sphere-fixed frame in the left and right view, respectively. However, although the initial guess for the period of P_3 is nearly commensurate with the P_2 orbit, the algorithm does not successfully achieve precie periodicity. In contrast, at the location marked by the red dot, a small maneuver is required to achieve velocity continuity, approximately equal to 0.0003 nondimensional units or 10^{-5} m/s for an ellipsoidal primary with the largest semi-major axis equal to $\alpha = 500$ m.

CONCLUSION

In an initial investigation of the dynamical behavior of a particle in the vicinity of a binary system comprised of small irregular bodies, the focus in this analysis is the exploration of trajectories for a massless third body in synchronous and non-synchronous ellipsoid-sphere systems. For synchronous systems, a suite of families of periodic libration point orbits are exploited to generate families of periodic orbits that visit the vicinity of all three equivalent collinear Lagrange points.

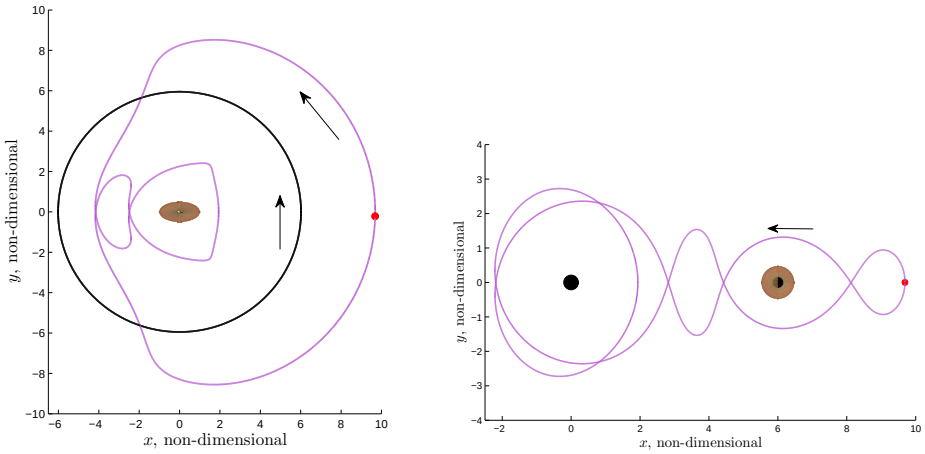

(a) Ellipsoid-fixed frame (b) Sphere-fixed frame

Figure 19. Non-synchronous double homoclinic cycle for $\beta = \gamma = 0.5 - \nu = 0.3 - r = 6$

Families of double heteroclinic cycles and double homoclinic cycles that offer close proximity passages with both primaries are produced. Incorporating a more complex model for the motion of the primaries, that is, for non-synchronous motion of the primaries, introduces additional challenges. However, the insight gained from the synchronous analysis is incorporated into a strategy to design trajectories that exhibit behavior that is similar to those constructed for the synchronous systems. In this investigation, only the gravitational forces that are exerted by an ellipsoidal and a spherical primary on a third body are included in the dynamical model. However, in the vicinity of small bodies, other disturbing effects, such as the solar radiation pressure, are not neglectable.

ACKNOWLEDGMENT

The authors are extremely grateful to Rune and Barbara Eliasen for their support of this research and funding for the Rune and Barbara Eliasen Visualization Laboratory at Purdue University.

REFERENCES

[1] R. W. Farquhar, D. W. Dunham, and J. V. McAdams, "NEAR Mission Overview and Trajectory Design, Special Issue on the Near Earth Asteroid Rendezvous Mission," *J. Astronautical Sciences*, Vol. 43, No. 4, 1995, pp. 353–371.

[2] M. D. Rayman, T. C. Fraschetti, C. A. Raymond, and C. T. Russell, "Dawn: A mission in development for exploration of main belt asteroids Vesta and Ceres," *Acta Astronautica*, Vol. 58, June 2006, pp. 605–616.

[3] M. Y. Marov, V. S. Avduevsky, E. L. Akim, T. M. Eneev, R. S. Kremnev, S. D. Kulikov, K. M. Pichkhadze, G. A. Popov, and G. N. Rogovsky, "Phobos-Grunt: Russian sample return mission," *Advances in Space Research*, Vol. 33, Jan. 2004, pp. 2276–2280.

[4] http://osiris-rex.lpl.arizona.edu/. Last accessed 02-23-2013.

[5] J. L. Margot, M.C. Nolan, L.A.M. Benner, S.J. Ostro, R.F. Jurgens, J.D. Giorgini, M.A. Slade, and D.B. Campbell, "Binary asteroids in the near-earth object population," *Science*, Vol. 296, 2002, pp. 1445–1448.

[6] P. Michel, M. A. Barucci, A. Cheng, H. Böhnardt, J. R. Brucato, E. Dotto, P. Ehrenfreund, I. Franchi, S. F. Green, L. M. Lara, B. Marty, D. Koschny, and D. Agnolon, "MarcoPolo-R: Near Earth Asteroid Sample Return Mission Selected for the Assessment Study Phase of the ESA program Cosmic Vision," *Acta Astronautica*.

[7] J. Bellerose and D. J. Scheeres, "Periodic orbits in the vicinity of the equilateral points of the restricted full three-body problem," *AAS/AIAA Astrodynamics Specialist Conference*, August 7-11 2005.

[8] J. Bellerose and D. J. Scheeres, "The restricted full three-body problem: Application to binary system 1999 kw4," *Journal of Guidance, Control, and Dynamics*, Vol. 31, No. 1, 2008, pp. 162–171.

[9] E. G. Fahnestock and D. J. Scheeres, "Simulation and analysis of the dynamics of binary near-Earth Asteroid (66391) 1999 KW4," *Icarus*, Vol. 194, 2008, pp. 410–435.

[10] E. G. Fahnestock and D. J. Scheeres, "Characterization of Spacecraft and Debris Trajectory Stability within Binary Asteroid Systems," *AIAA/AAS Astrodynamics Specialist Conference and Exhibit*, Honolulu, Hawaii, August 18-21, 2000.

[11] D. J. Grebow, "Generating Periodic Orbits in the Circular Restricted Three Body Problem with Applications to Lunar South Pole Coverage," M.S. Thesis, School of Aeronautics and Astronautics, Purdue University, West Lafayette, Indiana, May 2010.

[12] W. S. Koon, M. W. Lo, J. E. Mardsen, and S. D. Ross, "Heteroclinic connections between periodic orbits and resonance transitions in celestial mechanics," *Chaos*, Vol. 10, 2000, pp. 427–469.

[13] A. Haapala and K. Howell, "Trajectory Design Using Periapse Poincaré Maps and Invariant Manifolds," *21st AAS/AIAA Space Flight Mechanics Meeting*, New Orleans, Louisiana, February 2011.

[14] G. Gomez, J. Masdemont, and J. Mondelo, "Dynamical Substitutes of the Libration Points for Simplified Solar System Models," *Libration Point Orbits and Applications: Proceedings of the Conference, Aiguablava, Spain, 10-14 June 2002*, 2003, p. 373.

[15] X. Hou and L. Liu, "On quasi-periodic motions around the triangular libration points of the real Earth–Moon system," *Celestial Mechanics and Dynamical Astronomy*, Vol. 108, No. 3, 2010, pp. 301–313.

[16] X. Hou and L. Liu, "On quasi-periodic motions around the collinear libration points in the real Earth–Moon system," *Celestial Mechanics and Dynamical Astronomy*, Vol. 110, No. 1, 2011, pp. 71–98.